JOURNAL OF THERMOPHYSICS AND HEAT TRANSFER
Vol. 24, No. 2, April–June 2010

Experimental Investigation of Turbulent Heat Transfer in the Entrance Region of Microchannels

Tariq Ahmad,* Ibrahim Hassan,† and Ayman Megahed*
Concordia University, Montreal, Quebec H3G 1M8, Canada

DOI: 10.2514/1.36400

Within the entrance region of a closed channel, the effects on flowfield and heat transfer mechanisms are significant. Where microchannels and microdevices are concerned, there are limited heat transfer studies into this region, and those available are for laminar flows. In the turbulent regime, where the hydraulic resistance is conventionally increased, higher pumping powers are required. However, future microscale applications may have a need for turbulent flow data in microchannels. There is currently no heat transfer data available on the turbulent entrance region of microchannels. An experimental investigation has been carried out to explore turbulent convection heat transfer in the entrance region of uniformly heated microtubes. The measurement of local wall temperatures is achieved through the use of unencapsulated thermochromic liquid crystals, a state-of-the-art, nonintrusive thermal-measurement technique. Heat transfer data was obtained for two stainless steel microtubes, with nominal inner diameters of 1.067 and 0.508 mm, over a Reynolds number range of 4000 to 9000. The working fluid is FC-72, and adequate tube entry length is provided for hydrodynamic flow development before heating. Local temperature data and Nusselt values are obtained in the thermal entrance region of the microchannels. The thermal turbulent entrance length is found to remain relatively constant for the Reynolds number range considered for both microtube diameters. This is in good agreement with conventional thermal turbulent entrance studies for pipes.

I. Introduction

RECENTLY, a strong focus of the research community has been on fluid flow and forced convection heat transfer in microgeometries with and without phase change. Microgeometries consist of microchannels, which are prevalent in microdevices such as micro heat exchangers and micromixers. These are to be implemented in complete microsystems, like microengines and microreactors. However, before the advanced design of such systems, it becomes necessary to study the heat transfer and fluid flow characteristics of the integrated components. In addition, single-phase microchannel flow remains important in terms of applications, and there is a definite need for additional experimental investigations to understand the flow and heat transfer phenomena at the microscale.

The heat transfer in microchannels has important applications, such as the thermal control of electronic devices. Early studies, like that carried out by Tuckerman and Pease [1], show that electronic chips can be cooled effectively using forced convection by running water through microchannels mounted directly on the back of a circuit board. This initial study has led to continued research on microchannel heat transfer, which will eventually lead to the development of high-performance micro heat exchangers. These micro heat exchangers can have many applications: cooling of integrated circuits used in supercomputers and other high-density electronics, spacecraft thermal-management systems, and high-power-resistive magnets.

Numerous early experimental studies (Wu and Little [2], Pfahler et al. [3], Adams et al. [4], and Celata et al. [5]) on fluid flow and heat transfer in microchannels that were carried out for laminar and turbulent flows suggested there was disagreement from conventional theory for parameters such as friction factor, laminar-to-turbulent transition, and convective heat transfer coefficient. Papautsky et al. [6] stated that there are several experimental microscale effects that become important on the microscale level. Momentum transport effects and temperature variations can cause significant variations in fluid properties, leading to undetectable errors, undesirable levels of uncertainty, and complications in comparing microscale results with conventional theory. It can be seen that it is the early studies, as stated above, that indicate deviation from conventional theory, whereas recent studies (Owhaib and Palm [7], Lelea et al. [8], Lee et al. [9], and Muwanga and Hassan [10,11]) indicate good agreement with conventional theory for heat transfer and fluid flow in microchannels. The recent experimental studies have learned from past research efforts about the importance and accountability of experimental errors and uncertainties in microchannel flow, particularly with bulk measurements.

The majority of the studies carried out in past literature measure flow and heat transfer parameters with transducers, such as pressure sensors and thermocouples. These measurement devices measure bulk average properties within their immediate location, are intrusive in nature, create losses, and therefore have the possibility to create measurement errors and uncertainty of experimental data, particularly in the microdomain. Newer microscale techniques, like micro particle image velocimetry (micro-PIV), for fluid flow measurement (Santiago et al. [12], Meinhart et al. [13], Hao et al. [14], and Li and Olsen [15]), and thermochromic liquid crystals (TLCs), for temperature measurement (Ireland and Jones [16], Höhmann and Stephan [17], and Muwanga and Hassan [10,11]), are attractive in microscale studies due to their nonintrusiveness and high spatial resolution.

The entrance region, in which either the flow or the temperature profile (or both) are developing, can be very important, because the transport properties such as pressure gradient and heat transfer coefficient depend strongly on the flow region. It should also be stressed that general correlations for friction factor, heat transfer coefficient, and laminar-to-turbulent transition are only valid if the flow is fully developed. The hydrodynamic entrance length can be defined as the length from the inlet of a channel to a location over which the flow has attained 99% of its fully developed value, whereas the thermal entrance length can be defined as the length from the inlet of a channel to a location where the local Nusselt number is within 5% of its fully developed value (Shah and London [18]).

Very few laminar hydrodynamic entrance length studies were attempted in microgeometries (Lee et al. [19], Hao et al. [14], Lee and Kim [20], and Lee et al. [21]), with varying agreement with

Received 29 December 2007; revision received 26 July 2008; accepted for publication 26 July 2008.

*Department of Mechanical and Industrial Engineering.
†Department of Mechanical and Industrial Engineering; hassan@encs.concordia.ca.

conventional entrance length correlations. Also, laminar thermal entrance length studies, both experimental and numerical, were carried out (Lelea et al. [8], Muwanga and Hassan [10,11], and Lee and Garimella [22]), with the majority of the studies indicating very good agreement with conventional correlations.

It is widely conveyed that where practical applications are concerned, the majority of microsystem flows are laminar, due to the high pressure drop in microchannels caused by relatively small channel dimensions. In the turbulent regime, compared with laminar flow, the friction losses are conventionally increased, requiring very high pumping power to drive the flow. Nonetheless, future microscale applications may necessitate a need for turbulent-flow data in microchannels. To the authors' knowledge, there is currently no heat transfer data available on the turbulent entrance region of microchannels. A fundamental study of this nature is a novel and significant contribution in the area of microchannel heat transfer. Conventionally, turbulent thermal entrance length studies were carried out, both experimentally and numerically (Sparrow et al. [23], Malina and Sparrow [24], Notter and Sleicher [25], and Babus'haq [26]). It is fundamentally valuable to verify whether there is agreement between these conventional investigations and the turbulent thermal entrance length in microchannels.

The objective for the present study is to experimentally investigate the turbulent thermal entrance length, for developed hydrodynamic, turbulent-flow conditions. The study will be carried out for forced convective heat transfer in uniformly heated stainless-steel microtubes with nominal inner diameters of 1.067 and 0.508 mm, over a turbulent Reynolds number range from 4000 to 9000. The state-of-the-art unencapsulated TLC measurement technique for fine wall-temperature measurements in the thermal entrance region will be applied. TLC, as previously mentioned, is a nonintrusive thermal-measurement technique capable of full-surface mapping with a high spatial resolution, particularly in its unencapsulated form. Although the application of unencapsulated TLCs on a microchannel is challenging, these characteristics are attractive in resolving fine thermal entrance measurements.

II. Experimental Investigation

A. Test-Facility Flow Loop

The experimental flow loop used in the present study is shown in Fig. 1, and is the same used by Muwanga and Hassan [10,11]. This test facility was built to distinctly acquire TLC wall-temperature measurements of microchannels and microdevices, and was designed for both single-phase and flow boiling experiments. However, the present discussion will focus only on the elements required for single-phase flow. In regards to single-phase flow, the facility is capable of incorporating a number of different fluids to be analyzed, such as distilled water, a variety of refrigerants, and air. The working fluid in the present investigation is FC-72 (3 M), a low-viscosity electronics-cooling fluid widely used in industry ($Pr = 12.35$, $Cp = 1100$ J/kg°C, and $\mu = 6.4 \times 10^{-4}$ Ns/m^2 at room temperature).

The fluid operates in a closed system and is continuously circulated by means of a magnetically coupled gear pump (Cole-Parmer), as shown in Fig. 1. The gear pump operates at a controlled speed and supplies a maximum flow rate of 290 ml/ min, with a pressure of 517 kPa. Downstream from the pump is a 15 μm filter, to remove any particulates within the flow. The system flow rate was monitored by means of a nutating digital output flow meter (DEA Engineering), equipped to handle corrosive refrigerants. The flow meter outputs a 5 V square-wave signal at a frequency proportional to the time for the nutator to complete one cycle. Initial calibration of the flow meter was carried out using a precise weighing method and operates at a flow-rate range from 10–250 ml/ min. Before entering the microchannel test section, the fluid enters a preheater for additional flow-temperature control. The preheater is a counterflow, tube-in-tube heat exchanger, with distilled water as the heating fluid. As shown in Fig. 1, the test section is heated by means of Joule heating with the use of a power supply. Heater power was provided by a Good Will (GW) Instruments power supply (model GPC-1850) with a voltage range of 0–20 V and a maximum current rating of 10 A. Also apparent from the figure are the image and data acquisition systems, details of which will be explained in a later section.

B. Test Section

The present test sections used in evaluating the heat transfer characteristics in the thermal entrance region had the same manufacturing method for both the 1.067 and 0.508 mm microtubes. The primary test-section component is a circular cross-section microtube (Small Parts), manufactured from stainless steel. Figure 2 shows a schematic of the test section, which incorporates the microtube along with the plenum/measurement chambers. The nominal inner diameters (ID) of the microtubes are 1.067 and 0.508 mm, whose outer diameters (OD) are 1.27 and 0.635 mm, respectively. The hydraulic

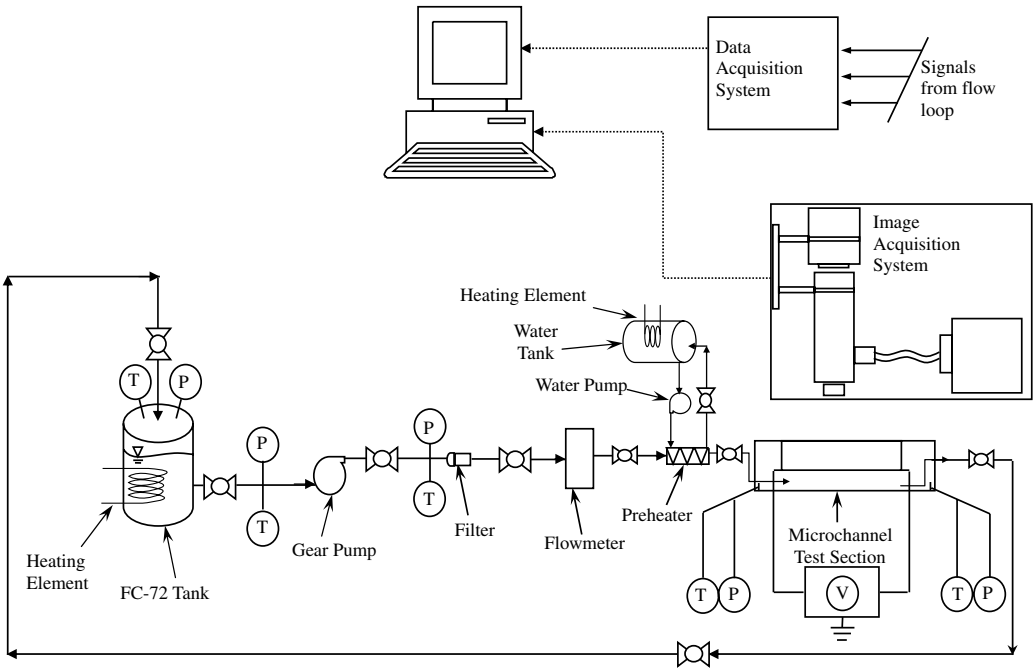

Fig. 1 Experimental test-facility flow loop.

length of both microtubes is 76 mm, and the heated length is 25 mm. Before the heated portion of the microtube, sufficient length was provided to assure hydrodynamic-developed flow throughout the heated length.

In manufacturing the test sections, shown in Fig. 2, a polycarbonate sheet was machined to produce the measurement chambers (inlet and outlet) for bulk pressure and thermocouple-temperature measurements. The tubes were connected to these chambers using standard 0.0625 mm stainless steel compression fittings with specialty ferrules to accommodate the small-diameter microtubes. Fabricated from a composite of graphite and polyimide, the ferrules have a high electrical resistance. Other advantages of using compression fittings are that they provide an excellent seal to both gas and liquid, can withstand high pressures (up to 690 kPa), and are resealable for repeated use. Copper stranded wire (14 AWG) was soldered at each end of the tube to provide the electrical lead connection necessary for Joule heating from the power supply. The inside edge of this lead connection provided a flat edge for the beginning of the heated length ($x \approx 0$), necessary for thermal entry length observation using the TLC measurement technique. There was no cover in direct contact with the TLC-coated surface of the microtube, due to the small diameter of the tube. To protect the TLC-coated surface from dust and room lighting, a noncontacting, optically clear plastic cover was placed over the tube.

C. Unencapsulated TLC Coating and Application

The measurement of local wall temperatures was achieved through the use of unencapsulated TLCs. Compared with conventional bulk-measurement techniques, such as thermocouples, TLC thermography is a nonintrusive thermal-measurement technique capable of full-surface mapping with a high spatial resolution, particularly in its unencapsulated form. Although there is a fair amount of difficulty regarding the application of unencapsulated TLCs on a microchannel, these measurement characteristics are attractive in resolving fine thermal-entrance measurements.

The application of TLCs can, in some cases, be a challenging endeavor. The TLCs should be applied as a uniform coating capable of producing vibrant colors for surface-temperature measurement. A thicker coating improves color vibrancy; however, if the coating is too thick, the coating itself can produce nonnegligible temperature gradients through the TLC layer. A relatively uniform application of the unencapsulated TLCs was applied through the use of an airbrush using a similar method as Muwanga and Hassan [10].

The unencapsulated liquid crystal material used is provided by LCR-Hallcrest. The TLC material nominally has a red-start of 40°C with a bandwidth of 10°C. The TLC material was applied onto the microtube surface using a Badger Model 100 independent-action airbrush. To provide an improved uniform layer of coating, the TLC material was dissolved in acetone with concentrations by weight of 20:1 (solvent to TLC). Before the application of the TLC coating on the microtubes, a water-based, black-paint coating was applied using the airbrush for improved color vibrancy of the TLC response.

D. Measurement Methods

Two 1.5 mm-diameter type-*T* (Omega special-limits-of-error material) thermocouples were placed in each plenum chamber of the test section (Fig. 2) to measure the bulk fluid temperature. Two static pressure transducers tracked the gauge pressure in the inlet and outlet plenums. The pressure transducers, both manufactured by Omega, are model PX01C1 at the microtube outlet and model PX02C1 at the microtube inlet, with ratings of 517 (75 psi) and 345 kPa (50 psi), respectively. The output from these and other sensors was monitored through an automated data-acquisition system using LabVIEW software. The data-acquisition hardware consisted of National Instrument's SCXI 1000 signal-conditioning unit, with the appropriate modules as well as the NI 6052E 16-bit 333 kHz data-acquisition card.

A schematic of the data-acquisition system is shown in Fig. 3. The signals from the transducers (pressure and temperature) were transferred through the signal-conditioning unit to reduce noise and improve signal strength, then through the data acquisition dAQ) card to the computer. However, signals from the metering devices (i.e., flow meter) were directly transferred to the computer through the DAQ card, without the use of the signal conditioner. Image acquisition was carried out in LabVIEW, and the images were captured in red-green-blue (RGB) format. The image size in pixels depends on the magnification and tube diameter. Hue planes were simultaneously extracted and saved in tagged image file format (TIFF). Image and data postprocessing was carried out using an in-house program in MATLAB.

A schematic of the image-acquisition system is shown in Fig. 4. Light from an illuminator box (Optem Intl.) is directed through a fiber-optic cable, keeping the heat generated from the light source away from the test section. The light from the illuminator box was meant to be passed through a polarizer before entering the zoom-lens casing, where it was to be deflected to the test surface by a beam splitter. However, even though the test facility has this capability, it

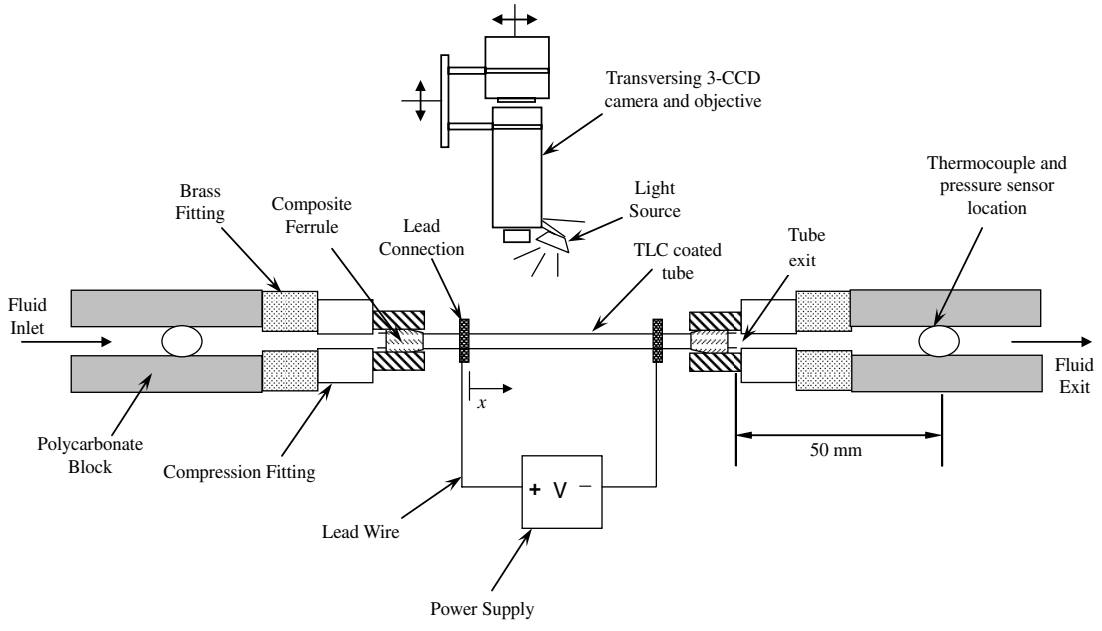

Fig. 2 Microtube test section used in present investigation.

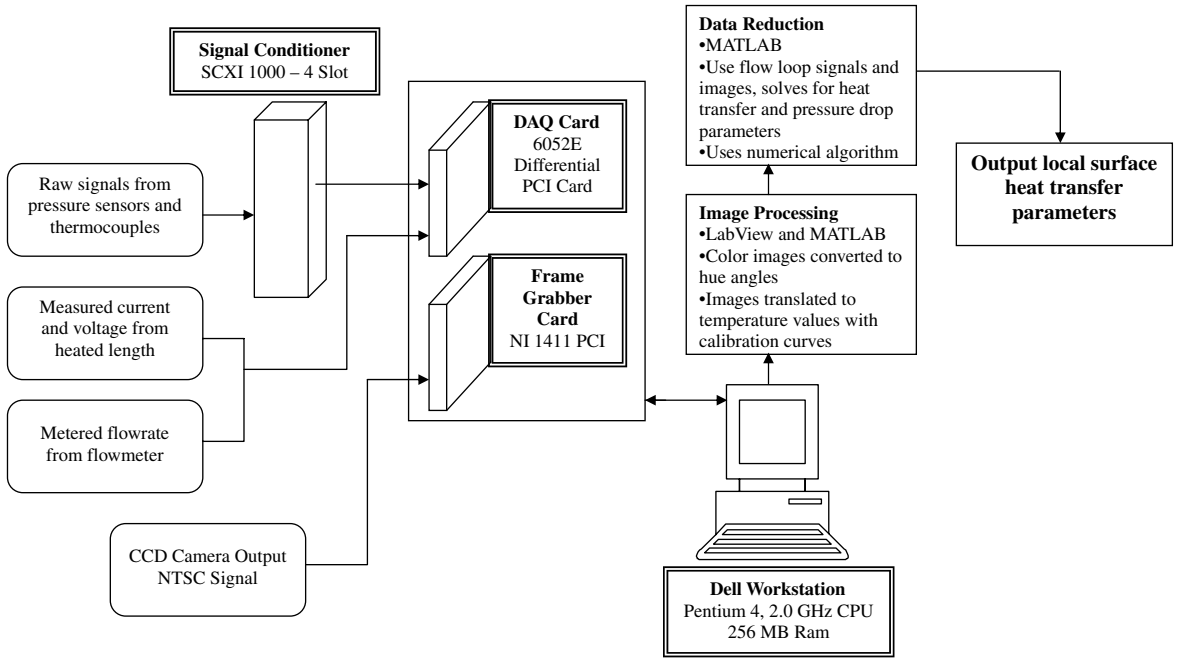

Fig. 3 Schematic of the data-acquisition system.

was not used in acquiring the microtube TLC images in the present study, due to the reduced intensity obtained when voltage was applied to the tube. Therefore, the fiber-optic illumination source directly illuminated the surface by fixing it onto the zoom lens at a fixed angle, as shown in Figs. 2 and 4. Upon reflection from the coated surface, the light is circularly polarized, passed into the zoom lens through the analyzer, and directed to the charged coupled device (CCD) camera. Since the reflected light is circularly polarized, it travels through the crossed polarizing pair unaffected. The acquired TLC image is then transferred directly to the computer as a NTSC signal through a BNC cable.

Through the use of an LCD television, real-time monitoring and positioning of the test section was possible. This allowed the operator to precisely align the test section as well as observe the colors of the TLC coated surface. The video signal used in the television loop comes from a separate output line directly from the camera. Image acquisition is obtained using a Sony 3-CCD analog camera, which is connected to a variable-zoom microscopic lens. This combination is mounted onto a three-axis traverse and equipped with variable-length stages with 1 μm resolution. The lateral and vertical-axis stages allow for fine-tuning of both focusing and positioning.

E. TLC Calibration

To acquire quantitative temperature data from TLC thermal colors on the surface of the microtube, it is required that the TLC material be calibrated to relate the observed color to a temperature value. There are many different available methods to quantify the observed color. In the present study, similar to Muwanga and Hassan [10,11], the hue angle was taken as the color descriptor. The hue angle, given by Hay and Hollingsworth [27], is defined as

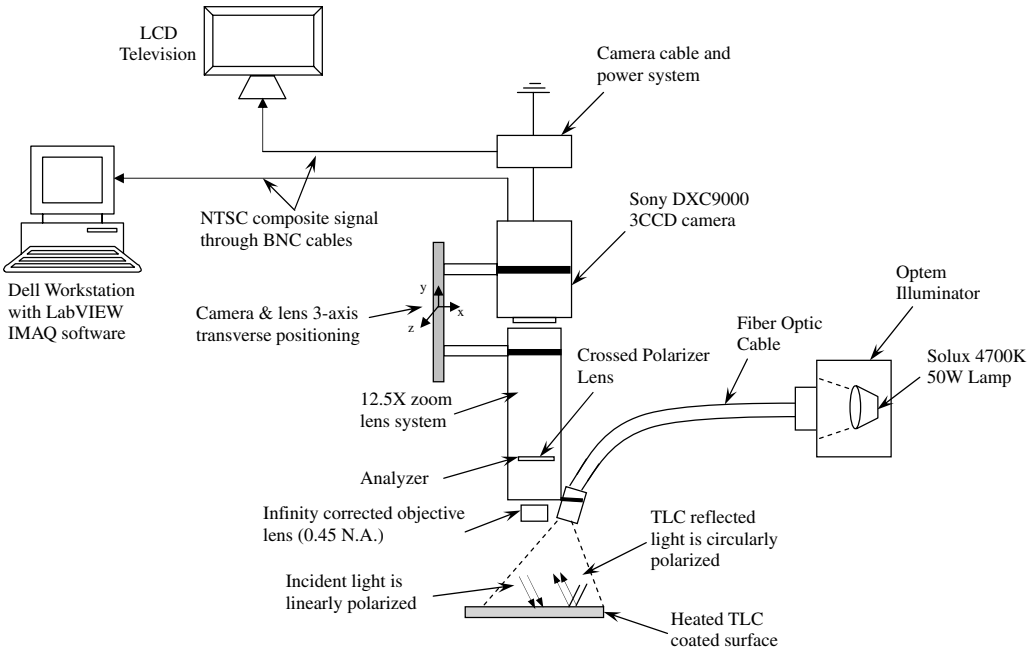

Fig. 4 Schematic of the image-acquisition system.

$$\text{Hue}\ (H) = \arctan\left(\frac{\sqrt{3}(G-B)}{2R-G-B}\right) \tag{1}$$

where R, G, and B are red, green, and blue values, respectively. The observed TLC color depends on many aspects, such as background lighting, camera distance, camera viewing angle, primary lighting angle and distance, and the time the TLC coating was applied to the specimen. In order for a valid and confident calibration to be carried out, all the above aspects must be maintained for both the calibration and the experiment.

The calibration is based on circulating the fluid through the channel and was selected due to its ease of incorporation into the setup. With the use of thermocouples, the bulk temperatures at the inlet and outlet of the channel were measured and remained within 0.5°C of each other. Through the use of the preheater, the fluid was slowly heated and images were captured at incremental changes in temperature, to cover the whole bandwidth of the TLC material (∼10°C). Also, since the present study dealt only with the thermal entrance region, only one axial position had to be recorded. This simplified the process, since there was no need to traverse the camera axially along the microtube.

Processing of the calibrated images was carried out as follows. Each calibration curve, which is a curve of hue angle vs temperature, represents a certain region of interest (ROI) on the tube surface. This eliminates aspects such as viewing angle and light distortion between different regions on the tube. Therefore, a size of the ROI must be selected. In the present study, a ROI of 4×3 pixels was selected, giving over 3000 calibration curves covering the entire image, depending on the tube size. The size of the ROI should be large enough to account for noisy pixels using statistics, but small enough to capture the local variability in the color change.

Through the use of MATLAB, an automated calibration curve fitting was utilized to fit the calibration data points. Initially a polynomial of order five was utilized to fit the points; however, if any local extensive fluctuations were present within a predefined region, the polynomial order was reduced to three. An example of this case is shown in Fig. 5a, which shows a calibration curve with the data points originally set at a fifth-order fit, then corrected to a third-order fit. Figure 5b shows a typical calibration curve that shows a good fit between the calibrated data and a fifth-order polynomial. Further details on the TLC calibration process can be found in (Muwanga and Hassan [10]).

F. Experimental Parameters and Procedure

Through the use of TLC thermography, wall-temperature data was obtained through images taken at a single measurement location for the thermal entrance region of the microtube's heated length. Forced convection experiments were carried out for both the 0.508 and 1.067 mm microtubes, and, regardless, the same calibration and measurement procedure was carried out for each test section.

Before each experiment, it was necessary to calibrate the coated TLC material, and since the experimental aspects (i.e., room lighting, test section position, etc.) must be maintained for both the calibration and measurements, the calibration and measurements were performed on the same day. It should also be noted that unless TLC images were being taken, the tube should remain covered (with a noncontacting cover) to reduce TLC degradation from exterior lighting. To begin the measurements, the flow rate was set and the system was allowed to run for about 10 min. Measurements were carried out for a flow range of 35–70 ml/ min for the 0.508 mm tube, and 85–155 ml/ min for the 1.067 mm tube. Using the preheater, the fluid temperature was raised until the inlet-fluid bulk temperature was just under the red-start of the TLC material (∼40°C). After running the flow through the system, measurements were ready to be taken and the protective noncontacting cover was removed. The illumination system was turned on, and the voltage from the power supply (Joule heating) was adjusted until the TLC color response was predominantly in the green range of the fully developed region (∼42–46°C). From observation, the color in the thermal entrance region was, for the most part, in the red range (∼39–42°C). The

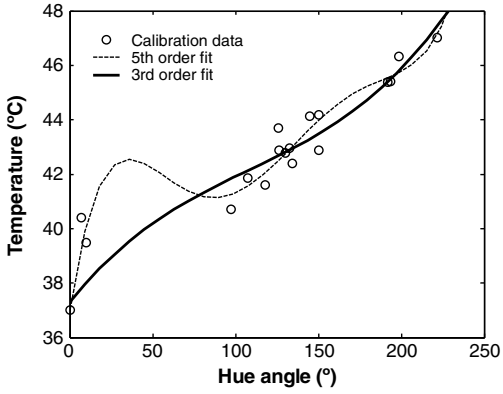

a)

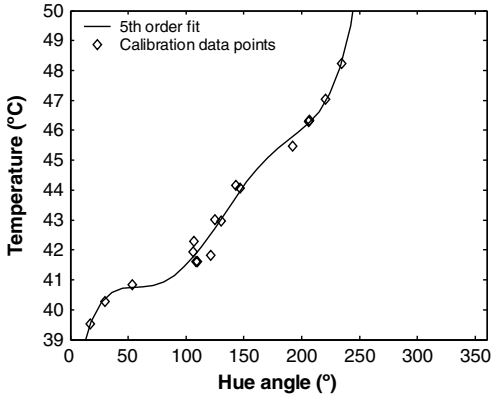

b)

Fig. 5 Examples of calibration curves: a) corrected calibration curve with third- and fifth-order fits and b) a typical good-fit calibration curve with a 5th-order fit.

system was allowed to come to equilibrium (5–10 min), after which a measurement image was taken.

Three color images were taken at a speed of 30 frames/s. Through the automated system, these images were converted to hue angle and scaled and then averaged for each pixel location. Simultaneously, the bulk fluid-temperature and gauge-pressure at the inlet and outlet, as well as flow-rate measurements were captured and recorded. Numerous images were recorded for each flow-rate and voltage setting; however, for data reduction, only the best images were selected for final presentation, based on visual inspection. Figures 6a and 6b show an example of raw RGB images for the 0.508 and 1.067 mm microtubes and their converted hue planes taken for the present investigation. From the figure, the turbulent thermal entry region is evident.

The experimental friction factor f_{exp} was obtained from the pressure drop ΔP relation:

$$\Delta P = \left(f_{\text{exp}}\frac{L_{\text{hyd}}}{D} + K_{\text{loss}}\right)\frac{\rho V^2}{2} \tag{2}$$

where L_{hyd} is the tube's hydraulic length, D is the microtube's inner diameter, ρ is the fluid's density, and V is the average velocity of the flow. The losses at the entrance and exit (K_{loss}) were estimated from Streeter [28], considering the area changes at each location between the pressure port and the tube entrance and exit. The heat flux to the fluid (q'') was calculated based on the fluid enthalpy change given by

$$q'' = \frac{\dot{m}Cp(T_{\text{out}} - T_{\text{in}})}{\pi D L_h} \tag{3}$$

where T_{out} and T_{in} are the outlet and inlet bulk fluid temperatures, respectively, and L_h is the heated length. The local heat transfer coefficient h_x was obtained through the convective heat transfer relation:

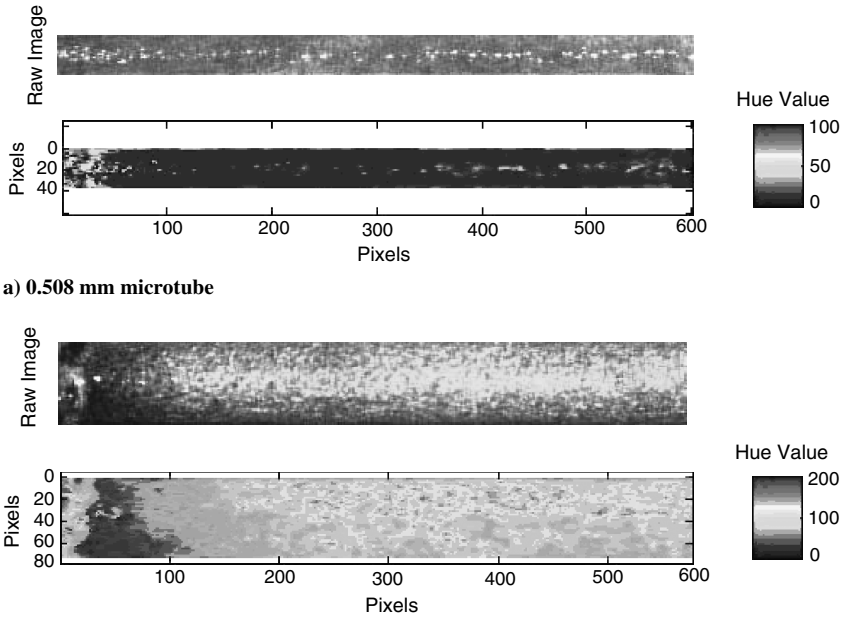

Fig. 6 Example of RGB raw images and their respective hue planes taken for the present investigation of the a) 0.508 and b) 1.067 mm microtubes.

$$h_x = \frac{q''}{(T_{w,xy} - T_{b,x})} \tag{4}$$

where $T_{w,xy}$ is the inner-wall temperature based directly on the TLC temperature measurement of the outer wall. $T_{w,xy}$ was estimated based on one-dimensional radial conduction (with heat generation) through the tube-wall thickness. It was found that the differences in the inner and outer wall temperatures were less than 0.3°C. $T_{b,x}$ is the local fluid bulk temperature, which was determined from an energy balance at each streamwise location given by

$$T_{b,x} = T_{\text{in}} + \frac{\pi D q''}{\dot{m} C p} x \tag{5}$$

The local Nusselt number Nu_x was calculated as

$$Nu_x = \frac{h_x D}{k_{\text{loc}}} \tag{6}$$

where k_{loc} is the local thermal conductivity of the fluid. Also, with a known volumetric flow rate Q, the Reynolds number Re was calculated as

$$Re = \frac{\rho Q D}{\mu A} \tag{7}$$

where μ is the fluid's dynamic viscosity and A is the microtube's inner cross-sectional area. Except for the local Nusselt number, the fluid properties for the above calculations were taken at the average fluid bulk temperature between the inlet and outlet. The properties of FC-72 were taken from the 3 M product information sheet.

G. Experimental Uncertainty

The uncertainty in TLC wall temperature depends on factors such as the sensitivity (slope) in the calibration curve (temperature vs hue angle), the uncertainty in the hue value, and the error in the polynomial curve fit of the calibration points. Wall-temperature uncertainty measurements were calculated using similar methods as Hay and Hollingsworth [27] and Muwanga and Hassan [10,11]. The wall-temperature uncertainty δT_w for an ROI can be calculated as

$$\delta T_w = \left[\left(\frac{\mathrm{d}T}{\mathrm{d}h} \delta h \right)^2 + \delta T_{\text{Fluid}}^2 + (2\text{SEE})^2 \right]^{1/2} \tag{8}$$

where $\mathrm{d}T/\mathrm{d}h$ is the sensitivity in the calibration curve, which can either be a third-order or fifth-order polynomial fit. The parameter δh is the uncertainty in hue for the ROI, and, since the ROIs were very small, a constant value of 1° was chosen, through visual observation, instead of the scatter. Also, an additional 2° was added to account for the conversion uncertainty from RGB to the composite signal. The parameter δT_{Fluid} is the uncertainty of the thermocouples used to measure the fluid bulk temperature at the inlet and outlet plenum chambers during calibration and was taken as 0.7°C. The standard error estimate (SEE), given by Hay and Hollingsworth [27], is defined as

$$\text{SEE} = \left[\frac{\sum_{i=1}^{n} [T_i(h) - T_{\text{fit},i}(h)]^2}{n - j - 1} \right]^{1/2} \tag{9}$$

The standard error estimate is a measure of the accuracy of the predicted polynomial used in fitting the calibration points and takes into account the error of the curve fit. However, it was noticed that since some calibrated points had large scatter, calculation of SEE was altered unreasonably. Therefore, instead of calculating SEE, a constant value of 0.5°C was selected for SEE based on repeated observations of the calibration curves. The uncertainty of the TLC wall temperature was found to be 1.1°C.

Experimental uncertainties were evaluated using standard methods outlined by Kline and McClintock [29]. The experimental uncertainties of typical parameters are tabulated in Table 1. Based on the manufacturer's instrument specifications, the uncertainties in the pressure drop and thermocouple measurements are ±0.73 kPa and ±0.7°C respectively. The uncertainty in flow rate was estimated at ±2.25 ml/ min, and typical local Nusselt-number uncertainty ranged from ±20 to ±30%. The high uncertainty in the local Nusselt number is due in part to the calculation of the heat flux to the fluid using an energy balance rather than using the power input from the power supply. However, using the change in enthalpy to calculate the heat-flux input is more accurate, because it eliminates the need to estimate the heat losses to the environment as well as the heat losses due to the resistance of the lead wires soldered to the tube. Uncertainties in the microtubes' inner and outer diameters are based on the manufacturing tolerance and are also given in Table 1.

III. Results and Discussion

Experimental data has been developed for turbulent convection heat transfer in the thermal entrance region of uniformly heated

Table 1 Uncertainty in parameters of the present study

Parameter	Uncertainty
Local Nusselt number Nu_x	20%–30%
TLC wall temperature Tw_x	1.1°C
Inlet/outlet temperatures T_{fluid}	0.7°C
Reynolds number Re	7.78%
Volumetric flow rate	±2.25 ml/ min
Microtube pressure drop ΔP	±0.73 kPa
0.508 mm microtube inner diameter ID	−0.0127 mm
0.508 mm microtube outer diameter OD	−0.0000 mm
1.067 mm microtube inner diameter ID	±0.0254 mm
1.067 mm microtube outer diameter OD	±0.0127 mm
Nondimensional axial distance x/D	16.20%

microtubes with inner diameters of 0.508 and 1.067 mm, over a turbulent Reynolds number range of 4000 to 9000. Sufficient tube entrance length (∼25 mm) was provided to assure hydrodynamic developed flow throughout the heated length. The cases that were considered for analysis were at $Re = 4717$, 6645, 7912, and 8733, for the 0.508 mm microtube, and $Re = 5399$, 6287, 8035, and 8926, for the 1.067 mm microtube. The measurement of local wall temperatures was achieved through the use of unencapsulated TLCs. The favorable characteristics of unencapsulated TLCs, such as full-surface mapping, high spatial resolution, and nonintrusiveness, are attractive in resolving fine thermal entrance measurements of a microchannel.

A. Pressure Drop

To assure the flow is indeed in the fully developed turbulent regime, the pressure drop was recorded over the microtube's length with the use of the inlet and exit static pressure transducers. From the experimental pressure drop, an experimental friction factor f_{exp} was obtained for both microtubes, using Eq. (2) for all Re numbers studied, and compared with a conventional turbulent Darcy friction factor, given by Filonenko [30] as

$$f = [1.82 \times \log(Re) - 1.64]^{-2} \tag{10}$$

Figure 7 shows the experimental friction factor for both microtubes studied, compared with Filonenko's [30] correlation. This correlation was selected due to its use in the average fully developed turbulent Nusselt number relation, as will be shown later. It can be seen that, for the most part, the correlation slightly underpredicts the experimental data. However, taking into account the experimental uncertainty of the pressure transducers, there is adequate agreement with Filonenko's [30] friction-factor correlation. Further, this data confirms that within the experimental Reynolds number range studied here (4000–9000), the flow is in the turbulent regime.

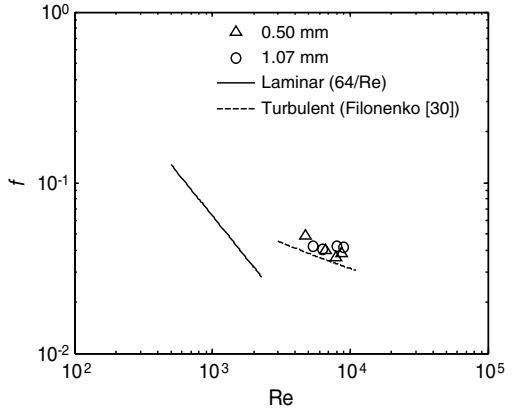

Fig. 7 Comparison of experimental friction factor with the Filonenko (1954) correlation.

B. Local Wall Temperature Measurements

Figures 8a–8d and 9a–9d depict the local wall temperature Tw_x along the nondimensional heated length x/D, from the inlet lead connection (see Fig. 2) of the 0.508 and 1.067 mm microtubes, respectively, for each Reynolds number studied. It should be pointed out that it was difficult to distinguish the exact physical point at which tube heating begins, even with the use of the high-magnification microscope apparatus. Identification of the heated length entrance was via visual selection of a pixel at the lead-to-tube contact. There is some uncertainty introduced by such a method; hence, the zero location of the tube lies in the vicinity of zero x/D, rather than exactly at zero. This can be seen on the x axis of Figs. 8 and 9. As can be seen, all figures show a similar trend in accordance with the developing temperature profile of a uniformly heated tube. Even though the cases presented in these figures show the dimensionalized local wall temperatures, which are dependant on the heat input, these figures serve to give a qualitative view of the trend of the wall temperature within the thermal entrance region.

In general, from conventional observations, due to the high forced convection effects, turbulent thermal entrance lengths are much shorter than laminar thermal entrance lengths. At the start of the heated length, the wall temperature is lowest; however, along the axial distance of the heated microtube, the local wall temperature increases dramatically, and then it becomes nearly constant at two to three microtube diameters. From the trend of data, it can be said that for all turbulent Reynolds-number test cases for both microtubes, the thermal entrance length is roughly two to three microtube diameters. In addition, since the heat input is, for the most part, variable for each case, the thermal entrance length is found to be independent of the heat flux. This indicates that for the Prandtl (Pr) number of our working fluid (FC-72, $Pr = 12.35$ at room temperature) and the Re range considered here (4000–9000), there is no effect on the thermal entrance length with turbulent Re number.

Conventionally, for turbulent flow, the higher the Prandtl number, the shorter the entrance length. However, there is a critical Pr number, above which the turbulence entrance length remains constant. This point is consistent with past researchers (i.e., Sparrow et al. [23], Malina and Sparrow [24], and Notter and Sleicher [25]) who modeled the turbulent thermal entrance length in conventional tubes for a uniform wall heat flux boundary condition. Although these models were for high Re numbers ($Re > 10^4$), impractical in their application to microflows, these researchers concluded that there is little influence of Re on the turbulent thermal entry length for high Pr numbers (greater than three). Regarding the local wall temperature for a developed temperature profile greater than two to three microtube diameters, it can be deduced that if the measurements were to extend along the axial distance of the tube throughout the entire heated length, one would observe a linear rise in the wall temperature, which is consistent for a fully developed temperature profile for a uniformly heated tube. Although measurements were confined to the thermal entrance region of the tube at low x/D values, in some cases this trend is apparent. Looking at Figs. 9a and 9b for the 1.067 mm tube, this trend is highly evident; however, from the 0.508 mm tube of Fig. 8, this trend is slight but detectable. From the local wall-temperature plots, it is evident that there is a fair amount of noise associated with the data. Since TLC is a local measurement technique with full-surface mapping, many data points can be obtained. A data point is obtained for each ROI, which is made up of only a few pixels. The data shown in the figures is downsampled from the raw data, as a data-reduction technique to obtain a viable trend. The scatter can be associated with the large amount of data points, as well as the uncertainty of the TLC measurement technique.

C. Validation in the Thermally Developed Region

The local Nusselt numbers along the microtube axial heated length x/D, for both the 0.508 and 1.067 mm tubes, are shown in Figs. 10a–10d and 11a–11d. These figures have similar implications as Figs. 8 and 9. The turbulent thermal entrance length at two to three microtube diameters remains constant for our working fluid and Re

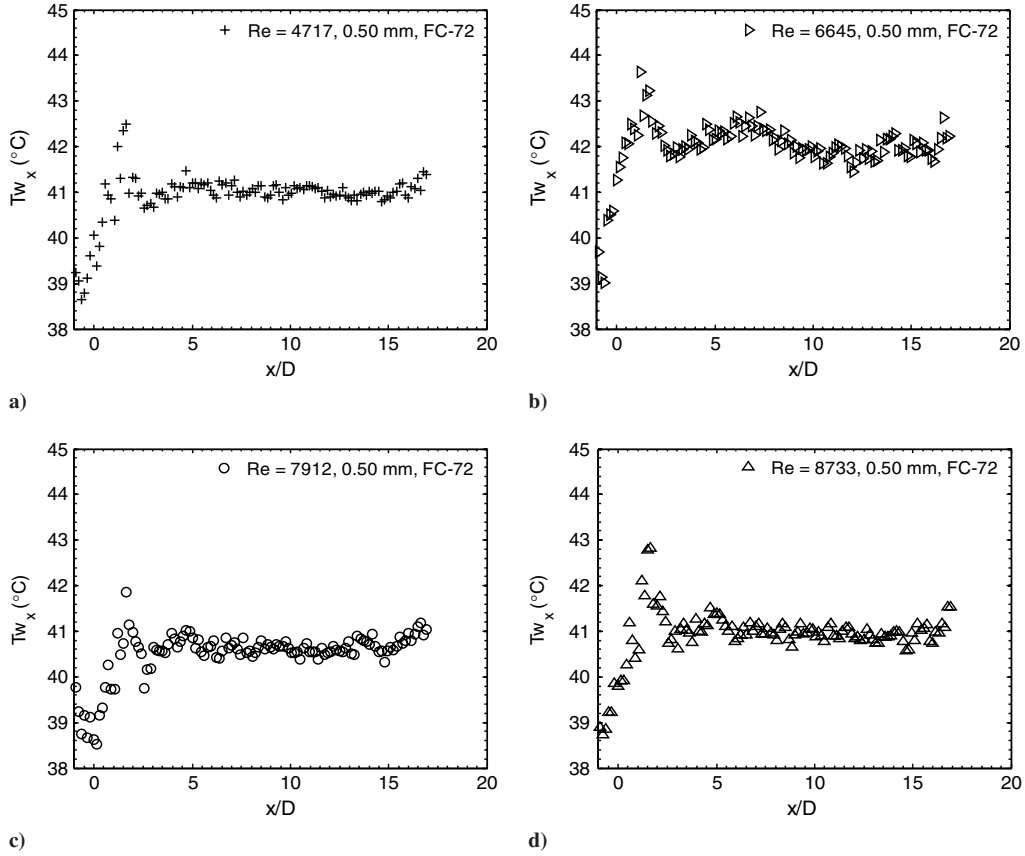

Fig. 8 Local wall temperatures at the thermally developing region of the 0.508 mm microtube for different Reynolds numbers of a) 4717, b) 6645, c) 7912, and d) 8733.

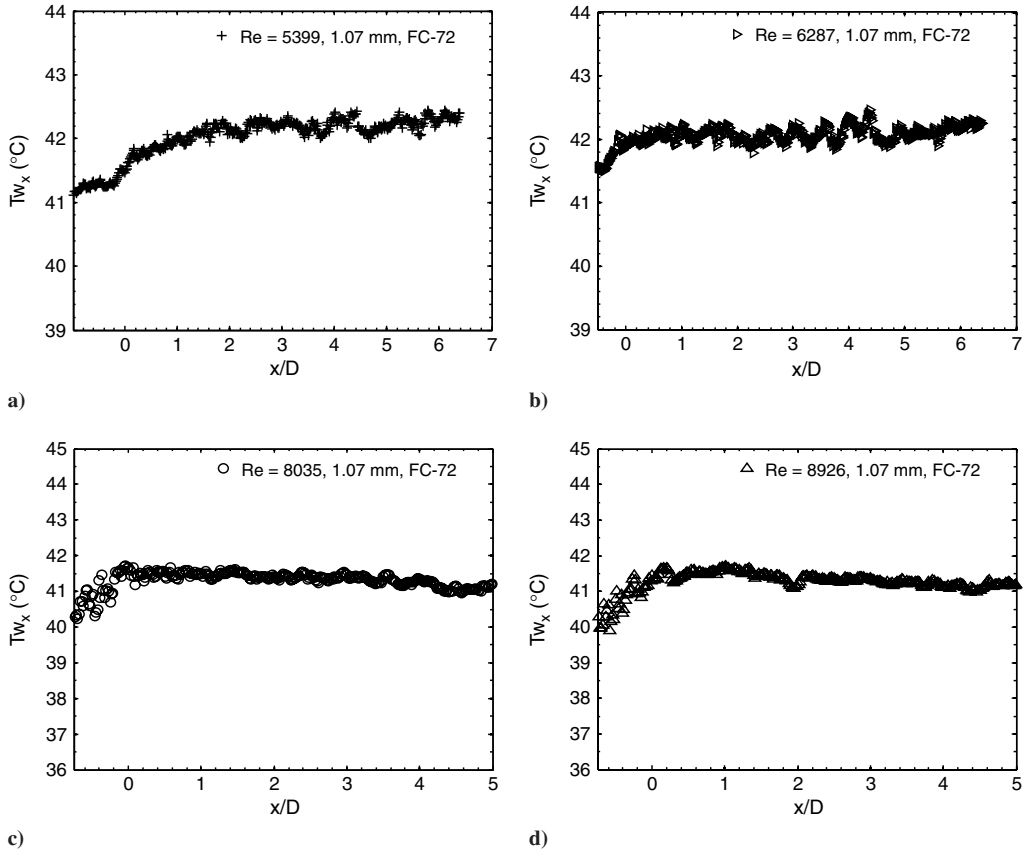

Fig. 9 Local wall temperatures at the thermally developing region of the 1.067 mm microtube for different Reynolds numbers of a) 5399, b) 6287, c) 8035, and d) 8926.

range considered here. Along with this, other similarities with the previous two figures include the presentation of the plots, the axial range of the data, and the scatter in the data.

However, the relative significance associated with these figures is the inclusion in the nondimensional analysis of the heat flux in presenting the Nusselt number, as well as validation of the analysis in the fully developed turbulent thermal region. Evident from the figures, the experimental data is compared with Gnielinski's [31] correlation for the average Nusselt number in the fully developed turbulent thermal region for large tubes, given by

$$Nu_{\text{Gniel}} = \frac{(f/8)(Re - 1000)Pr}{1 + 12.7(f/8)^{1/2}(Pr^{2/3} - 1)} \tag{11}$$

where Pr is the Prandtl number of the fluid, and the turbulent Darcy friction factor f is determined from Eq. (10). In solving Eq. (11), the fluid properties were taken at the average fluid bulk temperature between the tube inlet and outlet. Looking at Eq. (11), we see that Gnielinski's correlation is dependent not only on the Re and Pr numbers but also on the theoretical friction factor f. Also, Eq. (11) is valid for $0.5 \leq Pr \leq 2000$ and $2300 \leq Re \leq 5 \times 10^6$. This semi-empirical turbulent heat transfer correlation has some theoretical foundation, in that it is a combination of a functional form of a theoretically derived relation and empirically derived constants (Kays and Crawford [32]). According to Kakaç et al. [33], Eq. (11) is the recommended choice for turbulent heat transfer predictions in smooth tubes.

It can be seen from Fig. 10 that for the four Re test cases for the 0.508 mm microtube, there is very good agreement of the experimental local Nusselt number data with the conventional fully developed correlation given by Gnielinski [31]. From Fig. 11, for the 1.067 mm microtube, it is evident that there is very good agreement with Gnielinski at Reynolds numbers of 5399 and 6287 (Figs. 11a and 11b); however, there is large deviation for Re of 8035 and 8926 (Figs. 11c and 11d). The deviation associated with these two cases is possibly due to the applied heat flux. In the calculation of Gnielinski's correlation from Eq. (11), like many published correlations, the fully developed Nu number is found to be dependant on the Re and Pr numbers. Experimentally, the Nu number is dependant on the heat transfer coefficient, which in turn depends on the applied heat flux, although it should be noted that the error in Figs. 11c and 11d is within the uncertainty of the experimental Nusselt number.

The conformity in the comparison of the experimental Nusselt number with theory validates the present investigation in defining the turbulent thermal entrance length at two to three microtube diameters. The Nusselt number is highest in the entrance region, then levels out to a somewhat constant value in the fully developed region at this entrance length, which is consistent for all Re numbers analyzed. Also, since there is no available data similar to the present investigation, it shows that the trend of the data, from the start of the heated length through the turbulent thermal entrance region and towards the fully developed turbulent temperature profile, does indeed make physical sense. In addition, it lays emphasis that unencapsulated TLCs are a viable, valid, and attractive approach for wall-temperature measurements at the microscale, particularly due to its fine spatial resolution suited for microdimensions and its full-surface mapping capability to obtain a continuous trend of experimental data. These characteristics were advantageous for measurements within the turbulent thermal entry region.

D. Data Trend of the Thermally Developing Nusselt Values

In comparing the experimental Nusselt number trend of the 0.508 mm tube in Fig. 10 with that of the 1.067 mm tube of Fig. 11, it can be seen that although there is good agreement in the overall experimental data in terms of the thermal entrance length, there is a slight difference in the trend of the two figures. From Figs. 10a–10d, as the wall temperature is sharply increasing in the entrance region, the forced convection Nusselt number is sharply decreasing. It can be seen that there is a noticeable undershoot in the Nu data, after which

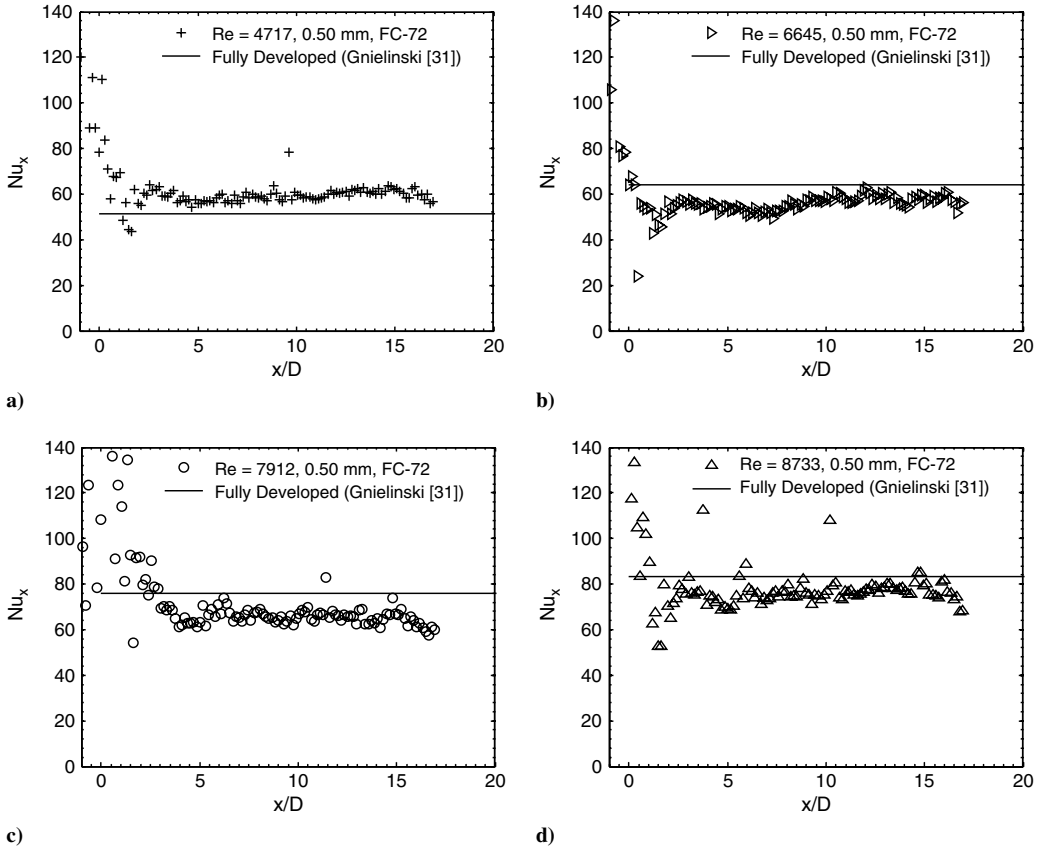

Fig. 10 Local Nusselt values at the thermally developing region of the 0.508 mm microtube for different Reynolds numbers of a) 4717, b) 6645, c) 7912, and d) 8733.

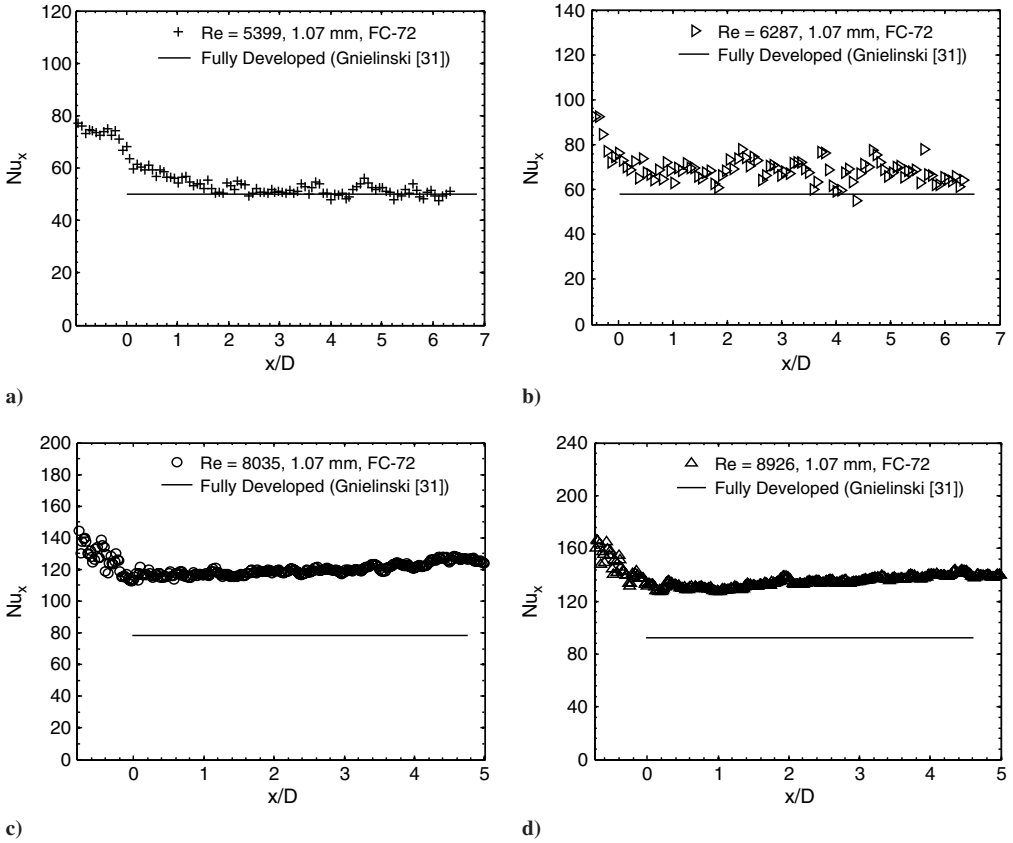

Fig. 11 Local Nusselt values at the thermally developing region of the 1.067 mm microtube for different Reynolds numbers of a) 5399, b) 6287, c) 8035, and d) 8926.

the data increases towards its fully developed value. This tendency is apparent for all Re cases for the 0.508 mm tube and is also evident for the wall-temperature measurements of Fig. 8, where an overshoot in the temperature data is evident. However, looking at Figs. 11a–11d for all Re cases of the 1.067 mm tube, there is no such occurrence: the experimental Nu number trend decreases sharply and smoothly with no undershoot in the data. This trend is also observed in the wall-temperature measurements of the 1.067 mm tube in Fig. 9.

At first it was thought that this was a possible microscaling effect that becomes evident at microscale dimensions but not at conventional geometries, as with the 1.067 mm tube. To clarify this issue and verify the repeatability in the TLC data, further turbulent thermal entrance region experiments were carried out in the 0.508 mm microtube. Figure 12 shows the local Nusselt number Nu_x versus the nondimensional heated length x/D, for two data sets for the 0.508 mm tube. The first data set, taken on 18 January 2007, for $Re = 4717$, is the same as that shown in Fig. 10a. The second data set was taken nearly seven months later on 8 August 2007, on the same test section, for $Re = 4200$. The difference in the experiments was that a new coating and calibration process was applied to the second data set. According to the authors, the minor dissimilarity in the Re numbers of the two data sets has a minor importance, and the Re values of 4717 and 4200 are close enough to compare the trend and the repeatability of the TLC data.

Both data sets have good agreement with Eq. (9) in their respective thermally developed regions; however, this is not shown in the figure for reasons of simplicity. It can be seen from Fig. 12 that there is very good repeatability in the data, in that both data sets show a definite entrance region spanning about two to three diameters, then level out to a constant Nu number in the fully developed region. However, it can be seen that there is a sharper negative slope for the 18 January case compared with the August 8th case, where the entrance region data has a smoother shape. Also, from the figure, it can be seen that there is no undershoot in the data for the 8 August case as is the case for the 18 January case. Therefore, due to this observation, it can be

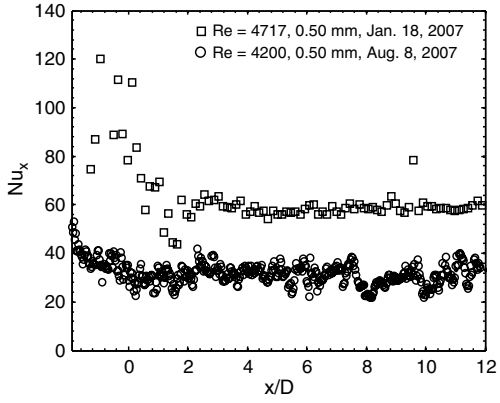

Fig. 12 Evaluation of the repeatability of the experimental results at similar turbulent Reynolds numbers.

said that the overshoot in the Tw_x data and the undershoot in the Nu_x data at the entrance region for the 0.508 mm tube (Figs. 8 and 10, respectively) are due to the TLC coating and not a scaling phenomena.

Figure 13 shows two trends of data of the local experimental Nusselt number Nu_x versus the nondimensional axial heated length x/D, for $Re = 5399$. The data is for the 1.067 mm microtube at two different heat fluxes of 1.345 and 0.784 W. This figure serves to demonstrate the dependence of the turbulent thermal entrance length on the heat input at a given turbulent Re number, where there is no distinct significance in the choice of the actual value of the flow rate. From the figure, it can be seen that, independent of the heat input, the turbulent thermal entrance length is at two to three diameters, consistent with the previous figures. This point further validates the present turbulent thermal entrance length analysis in that the entrance length is constant regardless of the heat flux and Re number for the

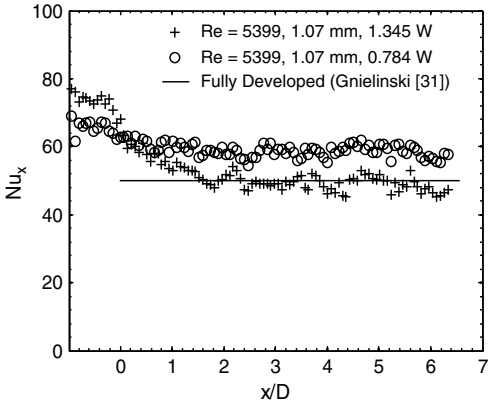

Fig. 13 Thermal entrance length comparison of two data sets with different heat power input and the same flow rate ($Re = 5399$).

Pr value studied. However, it is evident that there is a sharper drop (greater negative slope) in the local Nusselt number towards its fully developed value for the higher-heat-flux case of 1.345 W. This is expected, because a higher heat flux produces a higher local convective heat transfer coefficient. From Fig. 13, it can be seen that there is better agreement with the fully developed Nusselt value given by Gnielinski [31] for the higher-heat-flux case. However, the error associated with the lower heat flux case (0.784 W) is within the experimental uncertainty and is not critical.

IV. Conclusions

An experimental investigation into the turbulent thermal entrance region of uniformly heated microtubes was carried out. Experimental heat transfer entrance data was presented for two stainless steel microtubes with inner diameters 0.508 and 1.067 mm, over a turbulent Reynolds number range of 4000 to 9000. Sufficient microtube length was given to allow the flow to develop before heating. Therefore, turbulent thermal data was not obtained for simultaneously developing flow but for fully developed hydrodynamic flow developing thermally. The present fundamental experimental study was the first of its kind for flow in microchannels, with turbulent flow having possible future applications to microfluidics. High-resolution measurements of local wall temperatures were possible through the use of unencapsulated TLCs. TLC thermography is a nonintrusive surface-temperature measurement technique, possessing high thermal resolution and full-surface mapping in its unencapsulated form. These characteristics are attractive in analyzing microscale heat transfer phenomena, and the complete surface mapping allows the collection of continuous temperature data. The developing local wall temperature and local Nusselt number measurements showed good agreement with the physical mechanism describing thermally developing flow, and good agreement with conventional correlations was found in the thermally developed region of the microtubes. For the Reynolds number range considered, with $Pr \sim 10$ considering temperature effects), negligible variation in the entrance length was observed. The entry length was found to be two to three microtube diameters under the conditions considered, which is consistent with conventional studies. Further, it was demonstrated that unencapsulated TLCs are a viable approach for wall-temperature measurements at the microscale.

Acknowledgments

This research group has been funded by the Natural Sciences and Engineering Research Council of Canada. The authors would like to thank Roland Muwanga, a former member of the microscale Heat Transfer Research Group at Concordia University, for his guidance and efforts in the present study, particularly in the establishment of the experimental test facility and experimental methods, and for his experience, insight, and contributions into the area of research.

References

[1] Tuckerman, D. B., and Pease, R. F. W., "High-Performance Heat Sinking for VLSI," *IEEE Electron Device Letters*, Vol. 2, No. 5, 1981, pp. 126–129. doi:10.1109/EDL.1981.25367

[2] Wu, P., and Little, W. A., "Measurement of Friction Factors for the Flow of Gases in Very Fine Channels Used for Microminiature Joule–Thomson Refrigerators," *Cryogenics*, Vol. 23, No. 5, 1983, pp. 273–277. doi:10.1016/0011-2275(83)90150-9

[3] Pfahler, J., Harley, J., Bau, H., and Zemel, J., "Liquid Transport in Micron and Submicron Channels," *Sensors and Actuators, A: Physical*, Vol. 22, Nos. 1–3, 1990, pp. 431–434.

[4] Adams, T. M., Abdel-Khalik, S. I., Jeter, S. M., and Qureshi, Z. H., "An Experimental Investigation of Single-Phase Forced Convection in Microchannels," *International Journal of Heat and Mass Transfer*, Vol. 41, Nos. 6–7, 1998, pp. 851–857. doi:10.1016/S0017-9310(97)00180-4

[5] Celata, G. P., Cumo, M., Guglielmi, M., and Zummo, G., "Experimental Investigation of Hydraulic and Single Phase Heat Transfer in 0.130-mm Capillary Tube," *Microscale Thermophysical Engineering*, Vol. 6, No. 2, 2002, pp. 85–97. doi:10.1080/10893950252901240

[6] Papautsky, I., Ameel, T., and Frazier, A. B., "A Review of Laminar Single-Phase Flow in Microchannels," *Proc. ASME International Mechanical Engineering Congress and Exposition (IMECE2001)*, Vol. 3, ASME International Micro-Electromechanical Systems Div., New York, 11–16 Nov. 2001, pp. 495–503.

[7] Owhaib, W., and Palm, B., "Experimental Investigation of Single-Phase Convective Heat Transfer in Circular Microchannels," *Experimental Thermal and Fluid Science*, Vol. 28, No. 2, 2004, pp. 105–110. doi:10.1016/S0894-1777(03)00028-1

[8] Lelea, D., Nishio, S., and Takano, K., "The Experimental Research on Microtube Heat Transfer and Fluid Flow of Distilled Water," *International Journal of Heat and Mass Transfer*, Vol. 47, Nos. 12–13, 2004, pp. 2817–2830. doi:10.1016/j.ijheatmasstransfer.2003.11.034

[9] Lee, P.-S., Garimella, S. V., and Liu, D., "Investigation of Heat Transfer in Rectangular Microchannels," *International Journal of Heat and Mass Transfer*, Vol. 48, No. 9, 2005, pp. 1688–1704. doi:10.1016/j.ijheatmasstransfer.2004.11.019

[10] Muwanga, R., and Hassan, I., "Local Heat Transfer Measurements in Microchannels Using Liquid Crystal Thermography: Methodology Development and Validation," *Journal of Heat Transfer*, Vol. 128, No. 7, 2006, pp. 617–626. doi:10.1115/1.2193541

[11] Muwanga, R., and Hassan, I., "Local Heat Transfer Measurements on a Curved Microsurface Using Liquid Crystal Thermography," *Journal of Thermophysics and Heat Transfer*, Vol. 20, No. 4, 2006, pp. 884–894.

[12] Santiago, J. G., Wereley, S. T., Meinhart, C. D., Beebe, D. J., and Adrian, R. J., "A Particle Image Velocimetry System for Microfluidics," *Experiments in Fluids*, Vol. 25, No. 4, 1998, pp. 316–319. doi:10.1007/s003480050235

[13] Meinhart, C. D., Wereley, S. T., and Gray, M. H. B., "Volume Illumination for Two-Dimensional Particle Image Velocimetry," *Measurement Science and Technology*, Vol. 11, Part 6, 2000, pp. 809–814. doi:10.1088/0957-0233/11/6/326

[14] Hao, P.-F., He, F., and Zhu, K.-Q., "Flow Characteristics in a Trapezoidal Silicon Microchannel," *Journal of Micromechanics and Microengineering*, Vol. 15, Part 6, 2005, pp. 1362–1368. doi:10.1088/0960-1317/15/6/029

[15] Li, H., and Olsen, M. G., "MicroPIV Measurements of Turbulent Flow in Square Microchannels with Hydraulic Diameters from 200 μm to 640 μm," *International Journal of Heat and Fluid Flow*, Vol. 27, No. 1, 2006, pp. 123–134. doi:10.1016/j.ijheatfluidflow.2005.02.003

[16] Ireland, P. T., and Jones, T. V., "Liquid Crystal Measurements of Heat Transfer and Surface Shear Stress," *Measurement Science and Technology*, Vol. 11, Pt. 7, 2000, pp. 969–986. doi:10.1088/0957-0233/11/7/313

[17] Höhmann, C., and Stephan, P., "Microscale Temperature Measurement at an Evaporating Liquid Meniscus," *Experimental Thermal and Fluid Science*, Vol. 26, No. 2, 2002, pp. 157–162. doi:10.1016/S0894-1777(02)00122-X

[18] Shah, R. K., and London, A. L., *Laminar Flow Forced Convection in Ducts, Advances in Heat Transfer: Supplement 1*, Academic Press, New York, 1978.

[19] Lee, S.-Y., Wereley, S. T., Gui, L., Qu, W., and Mudawar, I., "Microchannel Flow Measurement Using Micro Particle Image Velocimetry," *Proceedings of the ASME International Mechanical Engineering Congress and Exposition*, New York, Vol. 258, ASME International Fluids Engineering Div., 17–22 Nov. 2002, pp. 493–500.

[20] Lee, S.-J., and Kim, G.-B., "Analysis of Flow Resistance Inside Microchannels with Different Inlet Configurations Using Micro-PIV System," ASME 1st International Conference on Microchannels and Minichannels, Rochester, NY, ASME International, Paper ICMM2003-1108, 21–23 Apr. 2003, pp. 823–827.

[21] Lee, S.-Y., Jang, J., and Wereley, S. T., "Entrance Length of Low Reynolds Number Flow in Microchannel," ASME International Mechanical Engineering Congress and Exposition (IMECE2004), Anaheim, CA, ASME International, FED, Paper IMECE2004-61908, 13–20 Nov. 2004, pp. 423–430.

[22] Lee, P.-S., and Garimella, S. V., "Thermally Developing Flow and Heat Transfer in Rectangular Microchannels of Different Aspect Ratios," *International Journal of Heat and Mass Transfer*, Vol. 49, Nos. 17–18, 2006, pp. 3060–3067. doi:10.1016/j.ijheatmasstransfer.2006.02.011

[23] Sparrow, E. M., Hallman, T. M., and Siegel, R., "Turbulent Heat Transfer in the Thermal Entrance Region of a Pipe with Uniform Heat Flux," *Applied Scientific Research A: Mechanics, Heat*, Vol. 7, Section A, 1957, pp. 37–52.

[24] Malina, J. A., and Sparrow, E. M., "Variable-Property, Constant-Property, and Entrance Region Heat Transfer Results for Turbulent Flow of Water and Oil in a Circular Tube," *Chemical Engineering Science*, Vol. 19, No. 12, 1964, pp. 953–962. doi:10.1016/0009-2509(64)85102-2

[25] Notter, R. H., and Sleicher, C. A., "A Solution to the Turbulent Graetz Problem 3: Fully Developed and Entry Region Heat Transfer Rates," *Chemical Engineering Science*, Vol. 27, No. 11, 1972, pp. 2073–2093. doi:10.1016/0009-2509(72)87065-9

[26] Babus'haq, R. F., "Forced Convection Heat Transfer in the Entrance Region of Pipes," *International Journal of Heat and Mass Transfer*, Vol. 36, No. 13, 1993, pp. 3343–3349. doi:10.1016/0017-9310(93)90015-X

[27] Hay, H. L., and Hollingsworth, D. K., "A Comparison of Trichromic Systems for use in the Calibration of Polymer-Dispersed Thermochromic Liquid Crystals," *Experimental Thermal and Fluid Science*, Vol. 12, No. 1, 1996, pp. 1–12. doi:10.1016/0894-1777(95)00013-5

[28] Streeter, V. L., *Handbook of Fluid Dynamics*, McGraw-Hill, 1st ed., 1961, pp. 3-8–3-22.

[29] Kline, J., and McClintock, F. A., "Describing Uncertainties in Single-Sample Experiments," *Journal of Mechanical Engineering Laboratory*, Vol. 75, Jan. 1953, pp. 3–8.

[30] Filonenko, G. K., "Hydraulic Resistance in Pipes," *Teploenergetika (Russia)*, Vol. 1, No. 4, 1954, pp. 40–44.

[31] Gnielinski, V., "New Equations for Heat and Mass Transfer in Turbulent Pipe and Channel Flow," *International Chemical Engineering*, Vol. 16, No. 2, 1976, pp. 359–368.

[32] Kays, W. M., and Crawford, M. E., *Convective Heat and Mass Transfer*, 3rd ed., McGraw–Hill, New York, 1993.

[33] Kakaç, S., Shah, R. K., and Aung, W., *Handbook of Single-Phase Convective Heat Transfer*, Wiley, New York, 1987.